

Kinematic Analysis and Simulation of an Orange Harvesting Robot

Sadaf Zeeshan (✉ sadafzeeshan6@gmail.com)

Assistant Professor, Mechanical Engineering Department, UCP, Lahore, Pakistan

<https://orcid.org/0000-0003-2776-9031>

Tauseef Aized

Professor, Mechanical Engineering Department, UET, Lahore, Pakistan

Original Article

Keywords: Kinematic analysis, path planning, trajectory, RoboAnalyzer, fruit harvesting robot

Posted Date: October 26th, 2020

DOI: <https://doi.org/10.21203/rs.3.rs-95136/v1>

License: © ⓘ This work is licensed under a Creative Commons Attribution 4.0 International License.

[Read Full License](#)

KINEMATIC ANALYSIS AND SIMULATION OF AN ORANGE HARVESTING ROBOT

Sadaf Zeeshan*, Tauseef Aized **

*Assistant Professor, Mechanical Engineering Department, UCP, Lahore, Pakistan <https://orcid.org/0000-0003-2776-9031>

**Professor, Mechanical Engineering Department, UET, Lahore, Pakistan <https://orcid.org/0000-0002-3820-6077>

Abstract

One of the most challenging areas in robot design is its kinematic analysis for proper and efficient path planning. In agricultural robots, this study is even more crucial due to the uneven terrain and unstructured environment. In agricultural robots, work has been done on fruit harvesting robots yet its commercial recognition is still underway. Further research needs to be done in this field to make the fruit harvesting robots more commercially acceptable. In this paper, a 6 degree of freedom (DOF) orange harvesting robot is designed and its kinematic analysis is done. Forward kinematic is done using Denavit-Hartenberg (DH) parameters while the inverse kinematics is done using algebraic method. The calculated formulas are verified by simulation on RoboAnalyzer software. The algorithm for inverse kinematics using probabilistic approach did not generate any error and worked successfully generating 16 results within the workspace. The simulated dynamic results also supported the kinematic model. The kinematic study validates the model design and calculations, whereas, its simulation verifies the path planning and reachability of oranges on the trees within the confined workspace.

Keywords: Kinematic analysis, path planning, trajectory, RoboAnalyzer, fruit harvesting robot

1. Introduction

With the improvement in technology and advanced sensors, robots have evolved as a major asset for our society. There is almost no field where robots have not made a mark for themselves. Where there are some fields conquered by automation, others are slowly advancing towards it. Agricultural sciences is also one such field which is very rapidly exploring the field of robotics for improvement and betterment of the agricultural systems. Some of the explored territory range from crop pest detection, environment monitoring, fertilizer spraying as well as fruit and vegetable harvesting (Juan Jesús Roldán, 2018).

Although agricultural sector has been working on robotics for some time now, there is still a large territory that needs to be explored. Many models of robots for fruit and vegetable harvesting were tested and research models have improved with time. However, many fruit harvesting robots are still not commercially acceptable worldwide (panelMichaelKassler, 2001). Unstructured terrain, maintaining fruit quality while picking, comparable pick up time as compared to humans and path planning are some areas that have been the focus of researchers for successful fruit and vegetable harvesting.

Many models of fruit harvesting robot have been designed. Fruit harvesting robots are usually designed for higher degree of freedom for easy access to all parts of the fruit. However, as the degree of freedom increase, the kinematic analysis for designing of the robot becomes more and more complicated especially for inverse kinematics. Kinematic study plays a vital role in trajectory and path planning of a robotic manipulator to reach its target object within the workspace. Forward kinematics helps determine the end effector position, whereas, the inverse kinematic study determines the joint angles that helps reach the end effector position and orientation without singularities.

Various methods for kinematics analysis studies have been done in the field of harvesting. Zhiyong Zou attempted the inverse kinematics for a watermelon for 5, 6 and 7 DOF (Zou, 2017). Youki also solved the inverse kinematics

for a 6 DOF robotic arm for path planning of apples using algebraic method (Yuki Onishi, 2019). Ali suggested 5 DOF kinematic analysis for crop harvesting like pumpkin and cabbage using geometric method for inverse kinematics (Roshanianfard, 2018). S. Parvathi (Parvathi, 2017) designed a 4 DOF robotic arm using inverse kinematic geometric calculations. E. Razzaghi used Jacobian method to do inverse kinematics for a 4 DOF date harvesting robot (E. Razzaghi, 2015). Sinem used analytical method for inverse kinematics of a 5 DOF robot for strawberry harvesting (Defterli, Oct 2017). Furthermore, Helena et al also did the kinematic study of a 5 DOF oil palm harvester using conventional Jacobian for the computation of velocity motion (Helena Anusia, 2010). Ma Guifei et al also attempted the inverse kinematics using Jacobian matrix and verified the results using ADAMS simulation software (Ma Guifei, 2010). Zhang Libin et al did the inverse kinematic study of a 4 DOF cucumber harvesting robot using inverse transformation technique (Zhang Libin, 2009). This paper presents the kinematic analysis of a 6 DOF model of an orange harvesting robot. The forward kinematics using DH parameters and inverse kinematic analysis using algebraic method for the designed model was computed and verified using RoboAnalyzer as its simulation tool.

This paper presents the kinematic analysis and simulation of a 6 DOF orange harvesting robot manipulator to see if the suggested calculations are viable for the proposed robotic model. **Section 4** covers the articulated robotic arm model design and the forward and inverse kinematics study. Modelling is done on SolidWorks. Forward kinematics is done using DH parameters while inverse kinematics is done using algebraic method for the designed orange harvesting robot manipulator. The workspace is defined such that manipulator is able to access the fruit at all points. In **section 5**, the forward and inverse kinematics is simulated and verified on RoboAnalyzer. Furthermore, the velocities and torques of the joints are also computed. The simulated model uses probabilistic approach to generate results for inverse kinematics that is used to validate the proposed model and to see if the study supports path planning of the robot to reach the fruit. The discussion and conclusion are presented in **section 6 and 7**, respectively.

2. Methodology

A 6 DOF articulated robot was designed for the purpose of orange harvesting. The model was designed on SolidWorks. For the proposed design, DH parameters were tabulated. Thereafter, transformation matrix was written for all the six joints. End effector position was determined by the combined effect of the transformation matrix. This completed the forward kinematic calculations. For inverse kinematics, algebraic method was used. Joint angles were computed for the six joints for the given end effector. RoboAnalyzer software was used to validate the forward and inverse kinematics. 16 solutions were generated for inverse kinematics for the given end effector position and orientation. The work space was also defined for fruit reachability. The torques and acceleration and velocities were also analyzed. Based on the results of kinematic analysis and dynamics, the path planning study is completed and the proposed model was proved viable for manufacturing.

3. SolidWorks Model

A 6 DOF manipulator model is drawn and assembled on SolidWorks. The model consists of aluminum manipulators with a pneumatic silicon soft gripper for prevent damage to orange while being picked. Servo motors are used and end effector is spherical with freedom to move in all directions.

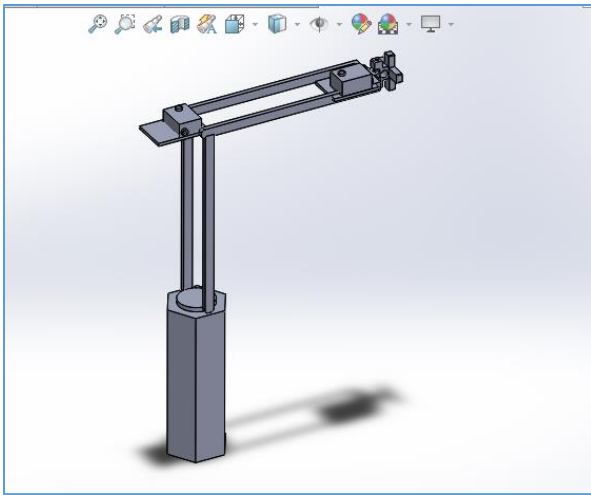


Figure 1: Model of 6 DOF orange harvesting robot manipulator on SolidWorks

4. Kinematic Study:

The kinematic study is divided into two parts. The first part deals with the forward kinematics that determines the position and placement of the end effector. The second part determines the positioning of the joints possible to support the end effector position. A 6 DOF robotic arm is designed with all revolute joints. The first three revolute joints consist of a waist, shoulder and the elbow that help with the positioning of the robotic arm end effector. The latter three joints comprise the wrist with three revolute joints that assist in the orientation of the end effector. The end effector is attached to a pneumatic soft gripper to assist in the fruit grasping without any damage.

4.1. Forward Kinematics:

The forward kinematics was done using the Denavit–Hartenberg parameters. The DH parameters use only 4 factors which describe the movement of the robotic arm. These parameters are:

- Θ : rotation angle/ this is along z axis always
- α : twist / this is the angle it takes to map z axis of previous joint to current joint
- a : distance of previous joint center to next center in x direction
- d (offset): distance of previous joint center to next in z direction

The diagram below shows the kinematic diagram of the robotic arm manipulator with 6 DOF. The parameters are determined for all the 6 joints.

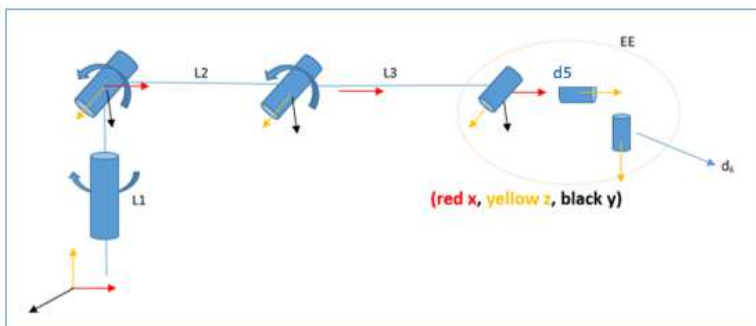


Figure 2: Kinematic diagram for 6 DOF robotic arm

Table 1: DH parameters for all 6 joints

	θ	A	A	D
1	Θ_1	90°	0.01	L1
2	Θ_2	0°	L2	0
3	Θ_3	-90°	L3	0
4	Θ_4	0°	0	0
5	Θ_5	90°	d_5	0
6	Θ_6	-90°	0	d_6

Next, using DH parameters, transformation matrix are written for each joint. For the designed robot mounted on a moveable plain, the link lengths for orange harvesting robot is as follows: $L_1=0.5$ m, $L_2=L_3=0.6$ m, $d_5=d_6=0.01$ m.

Homogeneous matrix that combines rotation and displacement movement as below:

$$T = \begin{bmatrix} R & d \\ 0 & 1 \end{bmatrix}$$

Therefore, the homogeneous matrix for each joint is given by keeping DH parameters of each joint in mind

$$T_i = R_{z,\Theta_i} D_{z,\Theta_i} D_{x,\Theta_i} R_{x,\Theta_i}$$

Therefore solving for each joint, we get,

$$T_1^0 = \begin{bmatrix} c1 & 0 & s1 & 0 \\ s1 & 0 & -c1 & 0 \\ 0 & 1 & 0 & L1 \\ 0 & 0 & 0 & 1 \end{bmatrix} \quad (1)$$

$$T_2^1 = \begin{bmatrix} c2 & -s2 & 0 & L2c2 \\ s2 & c2 & 0 & L2s2 \\ 0 & 0 & 1 & 0 \\ 0 & 0 & 0 & 1 \end{bmatrix} \quad (2)$$

$$T_3^2 = \begin{bmatrix} c3 & -s3 & 0 & L3c3 \\ s3 & c3 & 0 & L3s3 \\ 0 & 0 & 1 & 0 \\ 0 & 0 & 0 & 1 \end{bmatrix} \quad (3)$$

$$T_4^3 = \begin{bmatrix} c4 & 0 & s4 & 0 \\ s4 & 0 & -c4 & 0 \\ 0 & 1 & 0 & 0 \\ 0 & 0 & 0 & 1 \end{bmatrix} \quad (4)$$

$$T_5^4 = \begin{bmatrix} c5 & -s5 & 0 & d5 \\ s5 & c5 & 0 & 0 \\ 0 & 0 & 1 & 0 \\ 0 & 0 & 0 & 1 \end{bmatrix} \quad (5)$$

$$T_6^5 = \begin{bmatrix} c6 & 0 & -s6 & 0 \\ s6 & 0 & c6 & 0 \\ 0 & -1 & 0 & d6 \\ 0 & 0 & 0 & 1 \end{bmatrix} \quad (6)$$

Hence,

$$T_6^0 = T_1^0 T_2^1 T_3^2 T_4^3 T_5^4 T_6^5 \quad (7)$$

Solving the above gives:

$$T_6^0 = \begin{bmatrix} a11 & a12 & a13 & a14 \\ a21 & a22 & a23 & a24 \\ a31 & a32 & a33 & a34 \\ a41 & a42 & a43 & a44 \end{bmatrix} \quad (8)$$

The first three transformation matrix are for links 1, 2 and 3 whereas the latter three transformation matrix are for a spherical wrist. The links position can hence be defined by:

$$T_3^0 = T_1^0 T_2^1 T_3^2 = \begin{bmatrix} c1c23 & -c1s23 & -s1 & c1(L2 c2 + L3 c23) \\ s1s23 & -c1s23 & c1 & s1(L2c2 + L3 c23) \\ -s23 & -c23 & 0 & -(L2 s2 + L3 s23) \\ 0 & 0 & 0 & 1 \end{bmatrix} \quad (9)$$

Therefore, location of links to position end effector position is given by the x axis, y axis and z axis being: $c1(L2 c2 + L3 c23)$, $s1(L2 c2 + L3 c23)$ and $-(L2 s2 + L3 s23)$, respectively.

4.2. Inverse Kinematics:

We use kinematic decoupling for determining the joint angles. This involves two steps of inverse position kinematics that gives the location of the end effector and inverse orientation kinematics that determines the exact position the end effector is in. Thus, inverse position kinematics locates the center of wrist O_c , whereas, the inverse orientation kinematics computes R^3_6 .

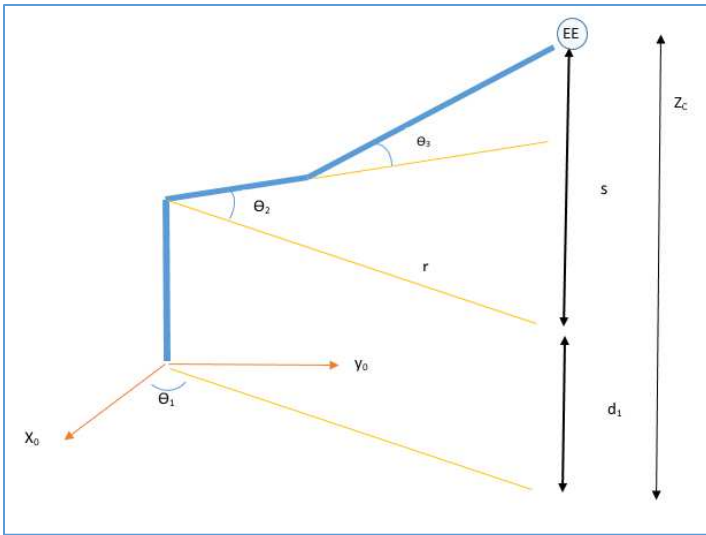


Figure 3: Angles and links of robotic arm manipulator for inverse kinematic study

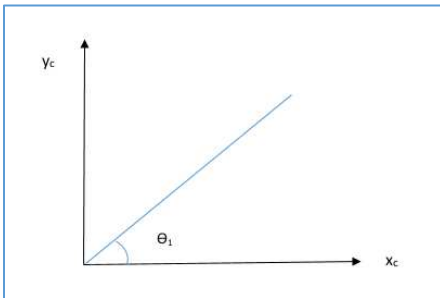


Figure 4: Projection on x-y plane

$$\tan\theta_1 = y_c/x_c$$

$$\theta_1 = \tan^{-1}y_c/x_c$$

Or

$$\theta_1 = \pi + \tan^{-1}y_c/x_c \quad (10)$$

From Figure 1, projection of manipulators on Link 1 plane gives:

$$r^2 = x_c^2 + y_c^2$$

Also, from Figure 1, projection of manipulators on Link 2 plane gives the below figure

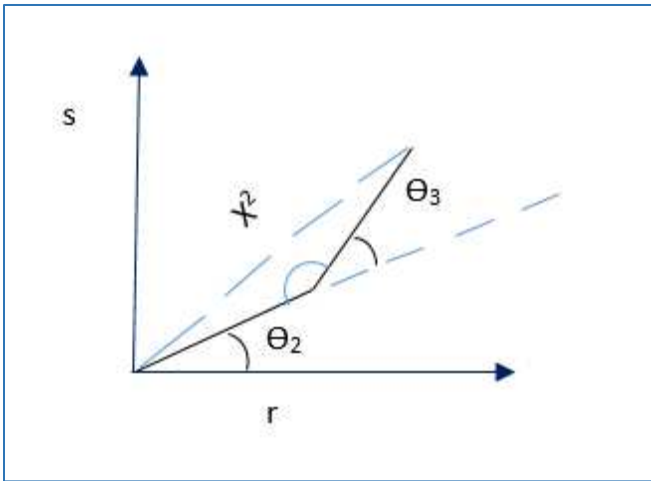


Figure 5: Projection on s-r plane

From cosine rule:

$$L_2^2 + L_3^2 - 2L_2 L_3 \cos\theta_3 = X^2$$

$$X = \sqrt{s^2 + r^2}$$

$$s^2 + r^2 = L_2^2 + L_3^2 - 2L_2 L_3 \cos\theta_3$$

$$\cos\theta_3 = \frac{s^2 + r^2 + L_2^2 - L_3^2}{2L_2 L_3} = D$$

$$\sin\theta_3 = \sqrt{1 - D^2}$$

$$\tan\theta_3 = \sin\theta_3 / \cos\theta_3$$

$$\tan\theta_3 = \sqrt{1 - D^2} / D$$

$$\theta_3 = \tan^{-1} \sqrt{1 - D^2} / D \quad (11)$$

Projection from side view shows

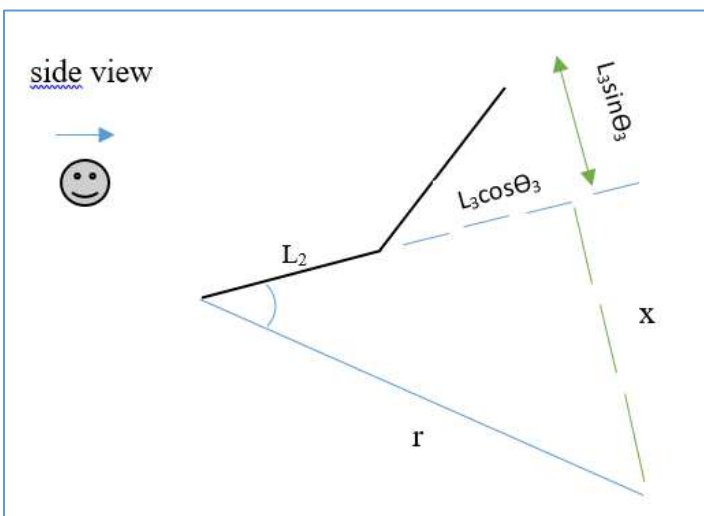


Figure 6: side view projection

$$\cos\theta_2 = \frac{x}{L_2 + L_3\cos\theta_3}$$

$$x = s - L_3\sin\theta_3$$

$$\tan\theta_2 = s - L_3\sin\theta_3/L_2 + L_3\cos\theta_3$$

$$\theta_2 = \tan^{-1} s - L_3\sin\theta_3/L_2 + L_3\cos\theta_3 \quad (12)$$

Hence, the joint angles are given by the formulas:

$$\theta_1 = \pi + \tan^{-1}yc/xc$$

$$\theta_2 = \tan^{-1} s - L_3\sin\theta_3/L_2 + L_3\cos\theta_3$$

$$\theta_3 = \tan^{-1} \sqrt{1 - D^2} / D \quad \text{where, } s^2 + \frac{r^2}{l_2^2} + L_3^2 - 2L_2 L_3 = D$$

This defines the position of the wrist and hence center Oc.

Now to define the orientation of the wrist, we consider the formula:

$$R^0_6 = R^0_3 R^3_6$$

Hence,

$$R^3_6 = [R^0_3]^T R^0_6$$

$$R^3_6 = \begin{bmatrix} c1c23 & s1s23 & -s23 \\ -c1s23 & -c1s23 & -c23 \\ -s1 & c1 & 0 \end{bmatrix} \begin{bmatrix} a11 & a12 & a13 \\ a21 & a22 & a23 \\ a31 & a32 & a33 \end{bmatrix}$$

Solving the above and simultaneously reveals,

$$\theta_4 = \text{atan2}(-c1s23a13 - s1s23a23 + c23a33, c1c23a13 + s1c23a23 + s23a33) \quad (13)$$

$$\theta_5 = \text{atan2}[\sqrt{1 - (s1a13 - c1a23)^2}, s1a13 - c1a23] \quad (14)$$

$$\theta_6 = \text{atan2}(s1a12 - c1a22, -s1a11 + c1r21) \quad (15)$$

Hence, the above calculations show the joint angles $\theta_1, \theta_2, \theta_3, \theta_4, \theta_5$ and θ_6 can be computed for a given end effector position in a work space.

5. Simulation On RoboAnalyzer

5.1. Validation of Forward Kinematics

The given parameters are entered for the given 6 DOF articulated robot on a simulation software, RoboAnalyzer. The results and visual plot behavior gives clear insight of its kinematic behavior. The DH parameters determined earlier are entered for a 6 DOF articulated robot. For the given input angles of joints, transformation matrix is formed for all 6 link and end effector position and orientation is determined and hence a trajectory is drawn.

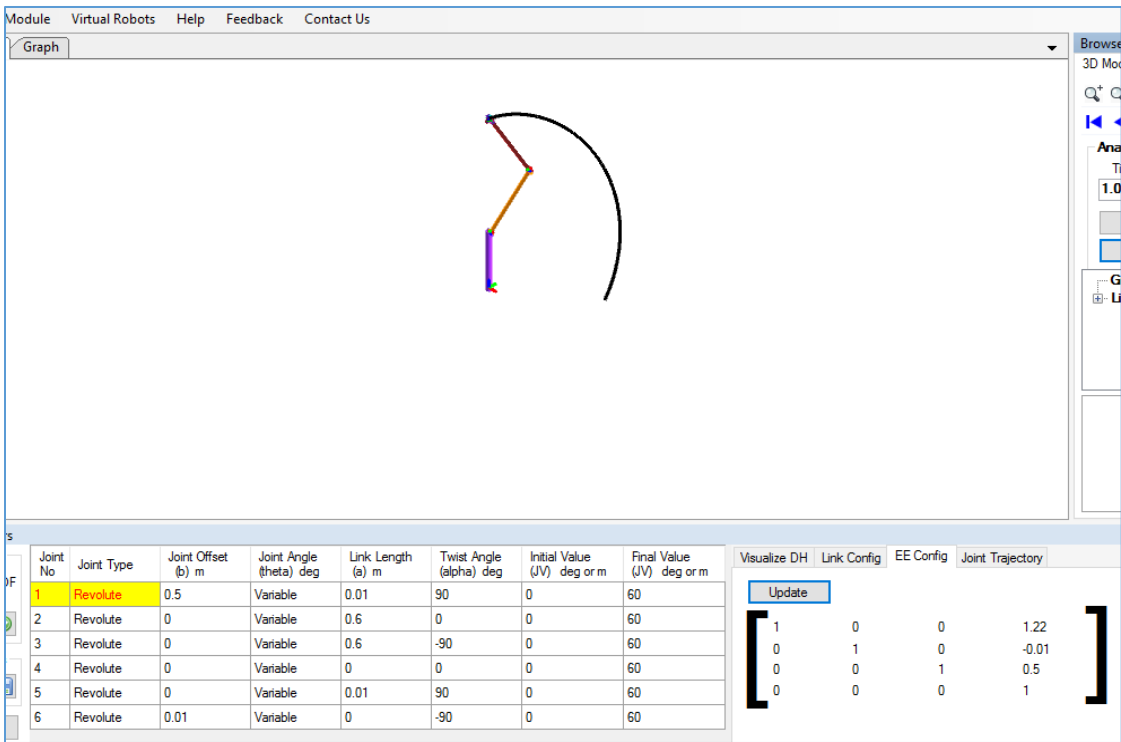


Figure 7: Forward Kinematics module in RoboAnalyzer for 6R manipulator

5.2.Workspace

The work space is the work envelope or the range of motion (ROM) of the robot. It consists of all the positions that the end effector can reach. For the above joint positions and link lengths, the work space is defined and illustrated as shown below such that it can access all the fruit on an orange tree.

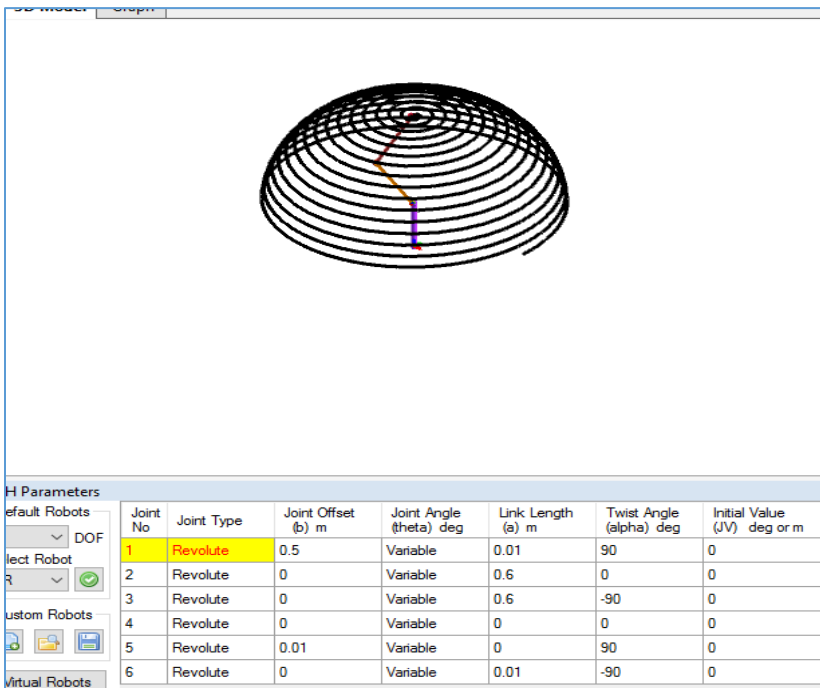


Figure 8: Workspace for the 6R manipulator on RoboAnalyzer

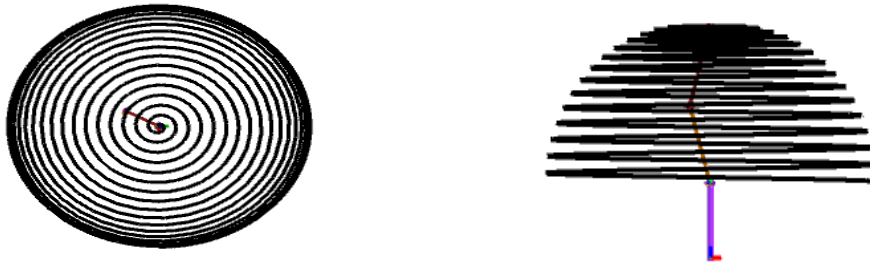


Figure 9: Top view and front view of the workspace

5.3.Validation of Inverse Kinematics

For inverse kinematics, there are three possibilities of outcomes. The first possibility may be that for the given end effector position and orientation, the inverse kinematics analysis may fail. Also, for the given end effector parameters, the object may be out of work space. This means that the end effector position chosen is beyond that scope of the workspace. The third possibility is that inverse kinematics is successful and several joint positions are possible for the given end effector orientation and position. The latter possibility is shown as “analysis complete” and results are generated. The following algorithm can be made for the inverse kinematic result possibilities as shown below:

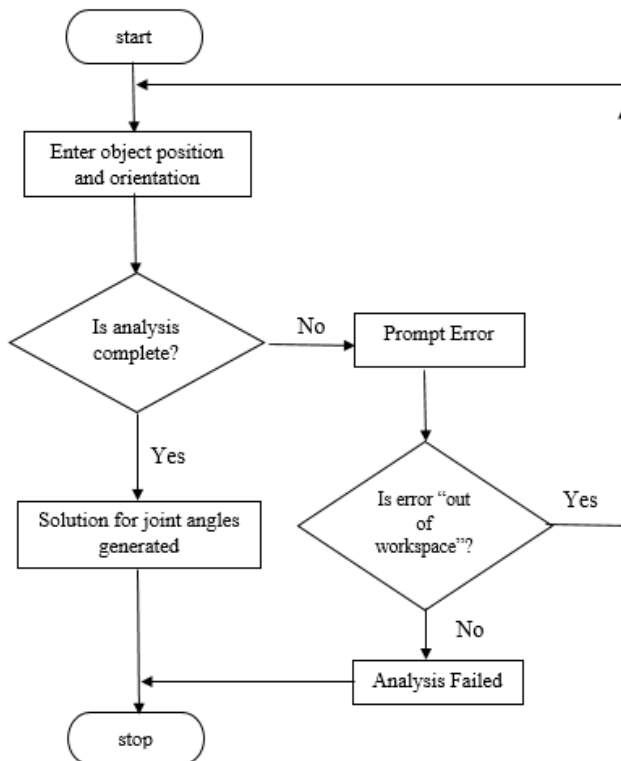


Figure 10: Inverse kinematics algorithm for RoboAnalyzer

For the above DH parameters, the results are generated and we see that 16 solutions are generated for the given end effector location and position.

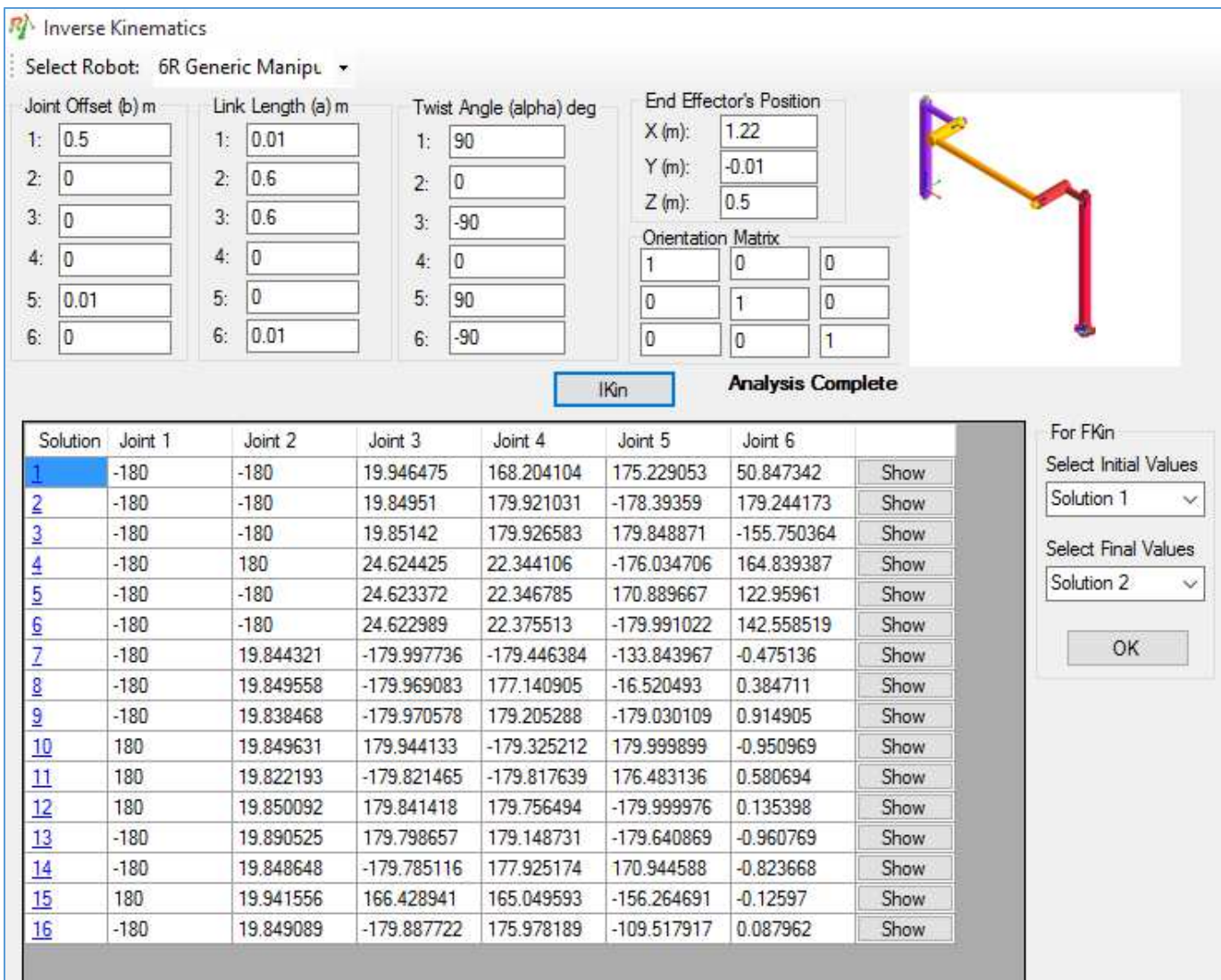


Figure 11: Inverse Kinematic Results for the given end effector position and orientation

This shows that for the given end effector position and orientation, the following angles for all six joints are possible for motion of the robotic arm. The comparison of the velocities and acceleration of joint angle is also given. The material of robotic arm and details also gives the comparison for values of the torques for a 6R robot. Sample result for velocities, acceleration and torques of joints are generated for one of the solutions of the kinematic analysis.

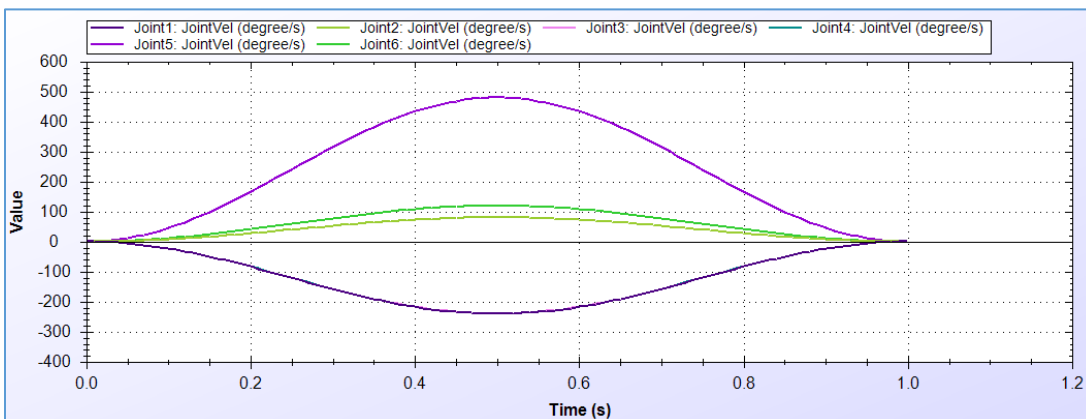


Figure 12: Comparison of all velocities of joints for 6R manipulator

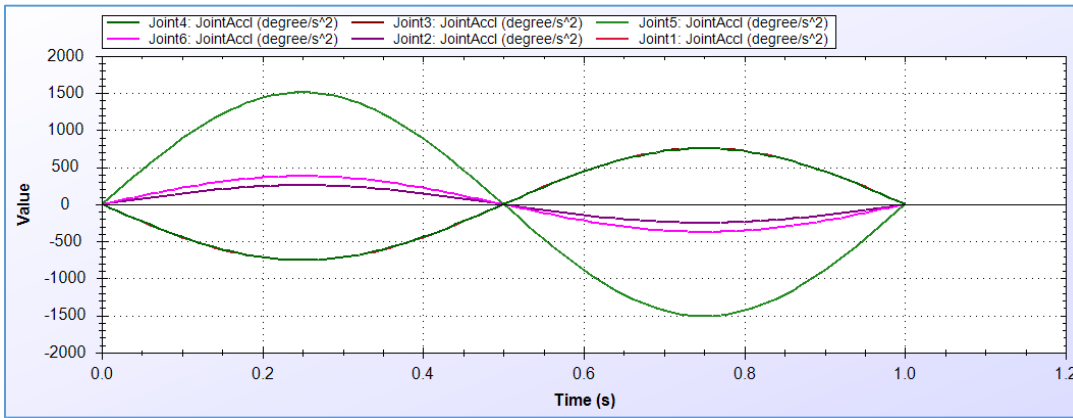


Figure 13: Comparisons of all accelerations of all 6 joints for 6R manipulator

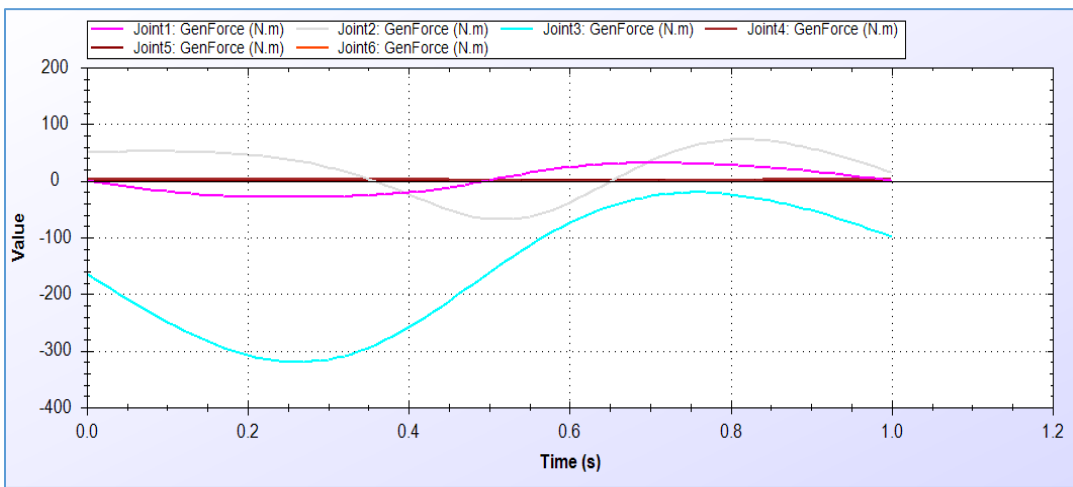


Figure 14: Comparison of torques of all joints for 6R manipulator

6. Discussion

According to the results of simulation, the kinematic study supports the successful motion of the robotic arms to reach the end effector within the workspace. The trajectory was accurate based on DH parameters. The workspace suggested good coverage of the orange tree. The inverse kinematics analysis was also successful and for the given algorithm generated 16 solutions for joint angles to reach the desired sample target fruit within the workspace. Furthermore, the dynamic study and graph generated on RoboAnalyzer for movement of the manipulators also supported the study. The results showed that proposed study could be successfully used for path planning for the purpose of orange harvesting.

7. Conclusion

Kinematic study of a high degree of freedom robot has always been a challenge. However, its importance can not be denied as it leads to the correct path planning of the robot. In this paper, kinematic study and simulation on RoboAnalyzer of a 6 DOF articulated robot is done for orange harvesting. The DH parameters were chosen for the design of an orange harvesting robot. 6 DOF is chosen for better reachability of fruit at various points. The forward kinematics is done by forming transformation matrix and determining the end effector position. The inverse kinematics is then done by using the end effector position and orientation as input and determining the various joint angles. Algebraic method is used to calculate the joint angles.

The simulation software RoboAnalyzer is used to verify the forward and inverse kinematic analysis. Forward kinematics is verified by simulation a trajectory for defined values. Algorithm using probabilistic approach for inverse kinematics is simulated on Roboanalyzer and maximum of 16 simulated results are achieved. Furthermore, the speed and acceleration of each joint is also determined. The workspace is also shown to define the reachability of orange on the tree. For the simulated model, dynamics is also studied and velocity and torque graphs are generated to further assist in the fabrication of the model.

Based on these results, one can conclude that kinematic calculations show that the 6 DOF robotic design works effectively. Smooth movement of robot is generated. Workspace gives a good coverage of the entire tree and fruit reachability is good. The robot is capable of reaching the designated position smoothly and effectively. The complete kinematic analysis hence verifies the calculated results and validates the path planning and reachability required for the designing of an orange harvesting robot within the workspace defined.

Declaration

Availability of data and material

The data that supports findings is available on request.

Competing interests

There are no competing interests

Funding

Not applicable

Author's Contribution

All authors contributed equally

Acknowledgement

This work is supported by ORIC, University of Engineering and Technology, Lahore, Pakistan and Mechanical Engineering Department of University of Engineering and Technology, Lahore, Pakistan.

8. References

1. Defterli, S. G. (Oct 2017). Analytical solution of a five-degree-of-freedom inverse kinematics problem for the handling mechanism of an agricultural robot. *International Journal of Mechanisms and Robotic Systems*, 4(1).
2. E. Razzaghi, J. M. (2015). Mechanical Analysis of a Robotic Date Harvesting Manipulator. *Russian Agricultural Sciences*, 41(1), 80-85.
3. Helena Anusia, J. J. (2010). Kinematics analysis for five DOF Fresh Fruit Bunch harvester. *IJABE*, 3(3).
4. Juan Jesús Roldán, J. d. (2018). *Robots in Agriculture: State of Art and Practical Experiences*. DOI:10.5772/intechopen.69874.
5. Ma Guifei, M. L. (2010). Apple Harvesting Robot Manipulator Kinematics Analysis and Simulation. *Journal of Agricultural Mechanization Research*.
6. Michael Kassler, (2001). Agricultural Automation in the new Millennium. *Computers and Electronics in Agriculture*, 30(1-3), 237-240.

7. Parvathi, S. (2017). Design and fabrication of a 4 Degree of Freedom (DOF) robot arm for coconut harvesting. *International Conference on Intelligent Computing and Control (I2C2)*. Coimbatore, India.
8. Roshanianfard, A. (2018). Kinematics Analysis and Simulation of A 5DOF Articulated Robotic. *Journal of Agricultural Sciences*, 24, 91-104.
9. Yuki Onishi, T. Y. (2019). An automated fruit harvesting robot by using deep learning. *ROBOMECH Journal, Springer*, 6(13).
10. Zhang Libin, W. Y. (2009). Kinematics and trajectory planning of a cucumbrer harvesting robot manipulator. *International Journal of Agricultural and Biological Engineering*.
11. Zou, Z. (2017). Research on the inverse kinematics solution of robot arm for watermelon picking. *IEEE 2nd Information Technology, Networking, Electronic and Automation Control Conference (ITNEC)*. Chengdu, China.

Figures

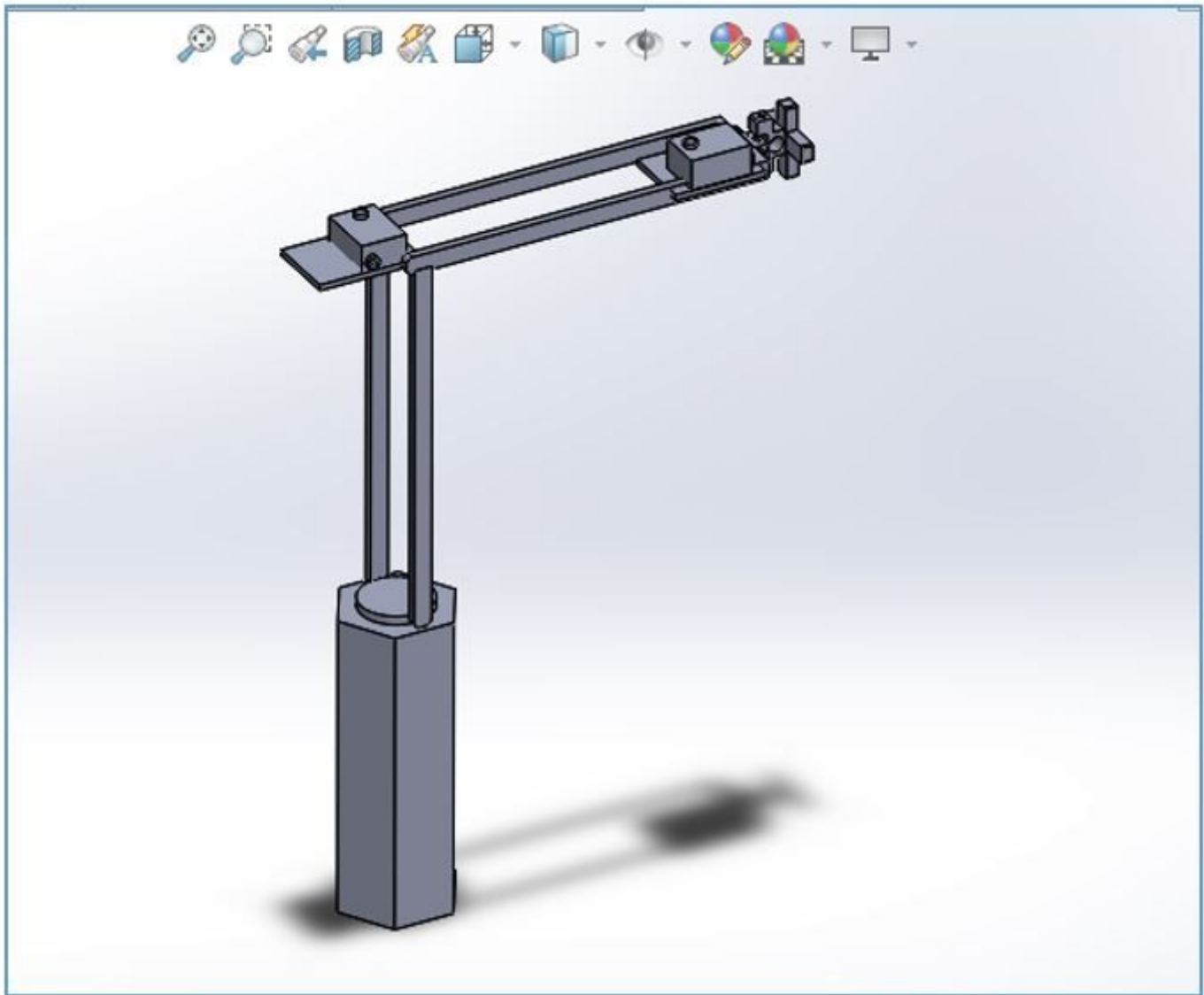


Figure 1

Model of 6 DOF orange harvesting robot manipulator on SolidWorks

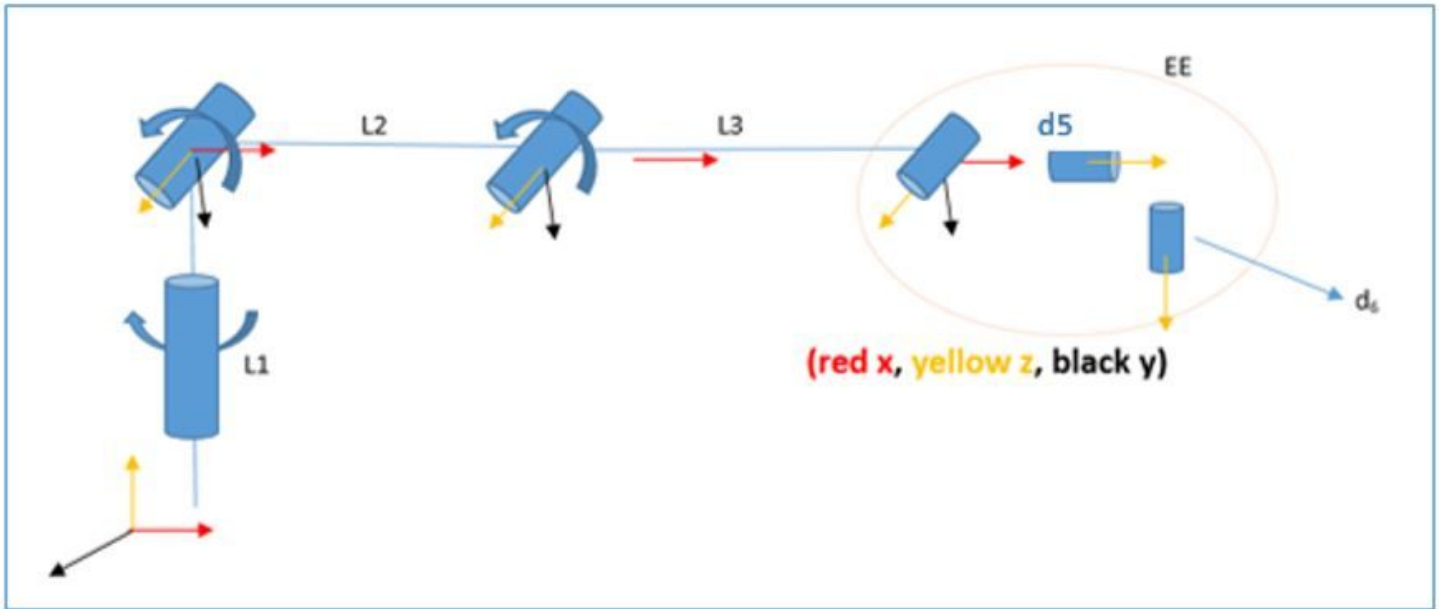


Figure 2

Kinematic diagram for 6 DOF robotic arm

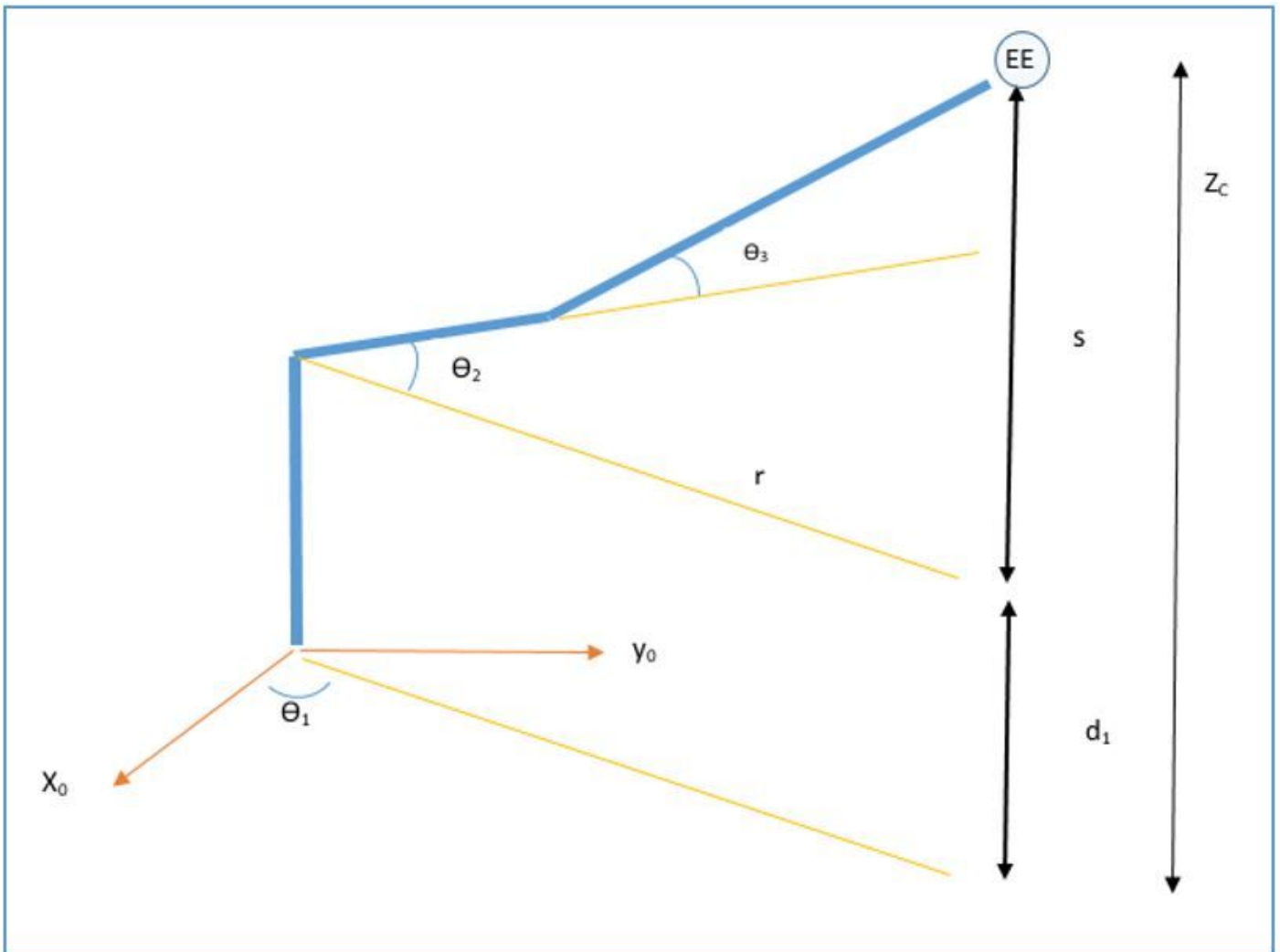


Figure 3

Angles and links of robotic arm manipulator for inverse kinematic study

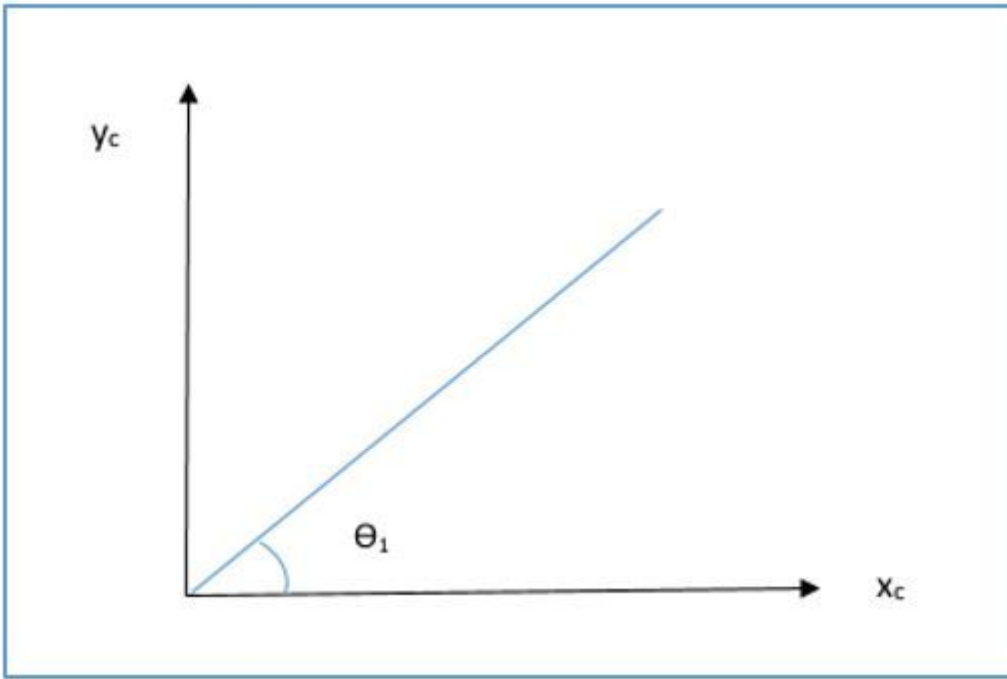


Figure 4

Projection on x-y plane

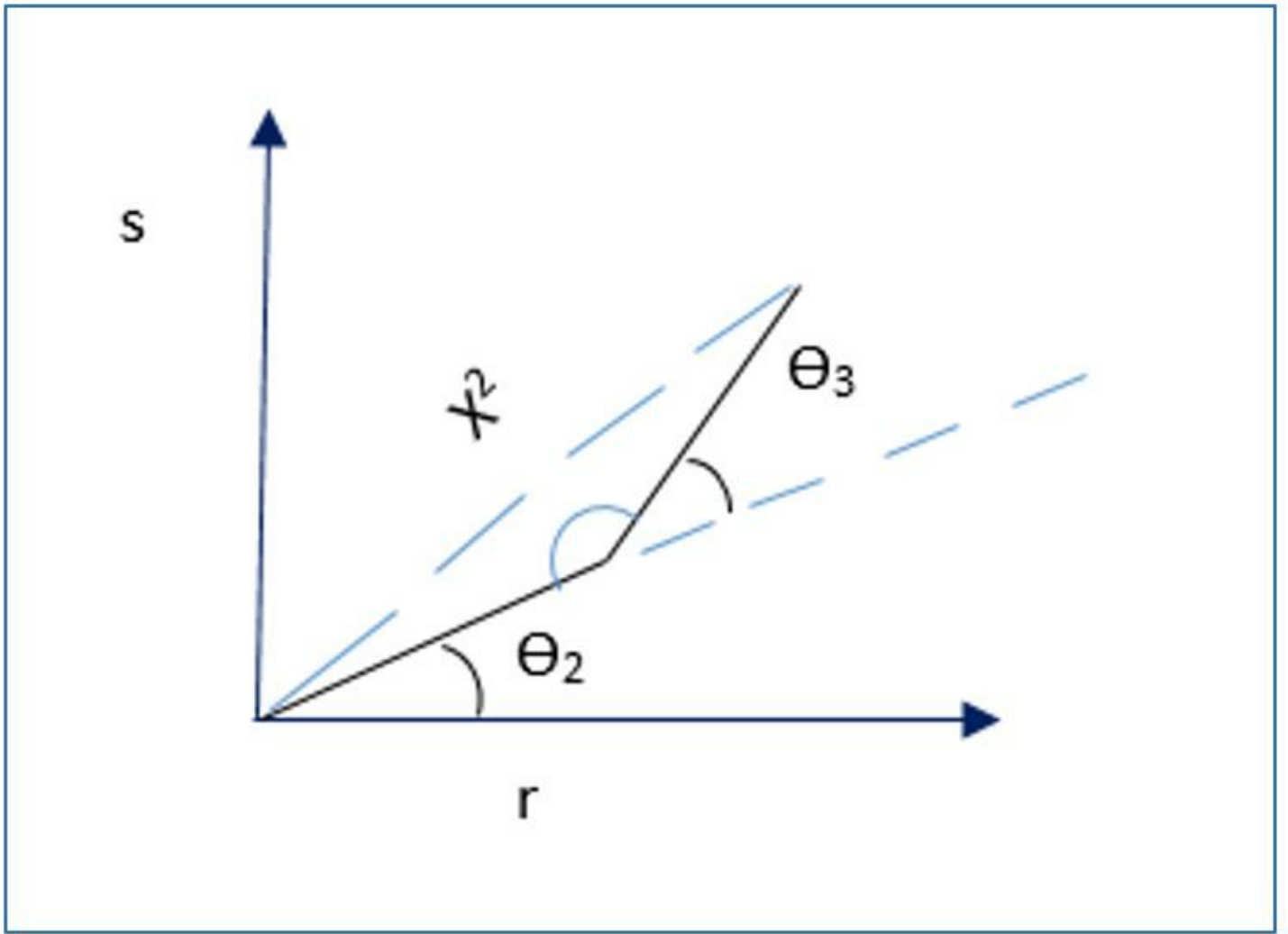


Figure 5

Projection on s - r plane

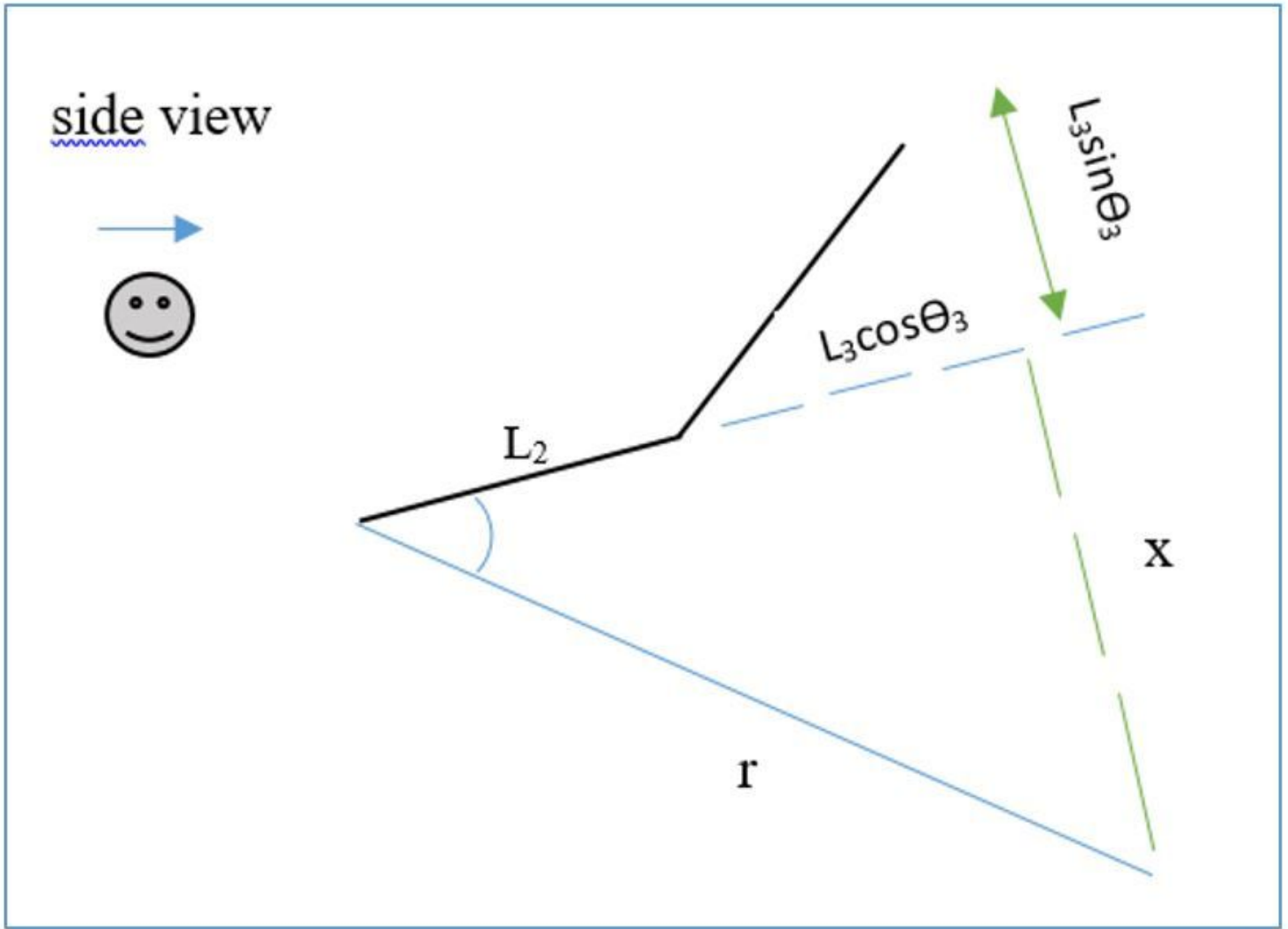


Figure 6

side view projection

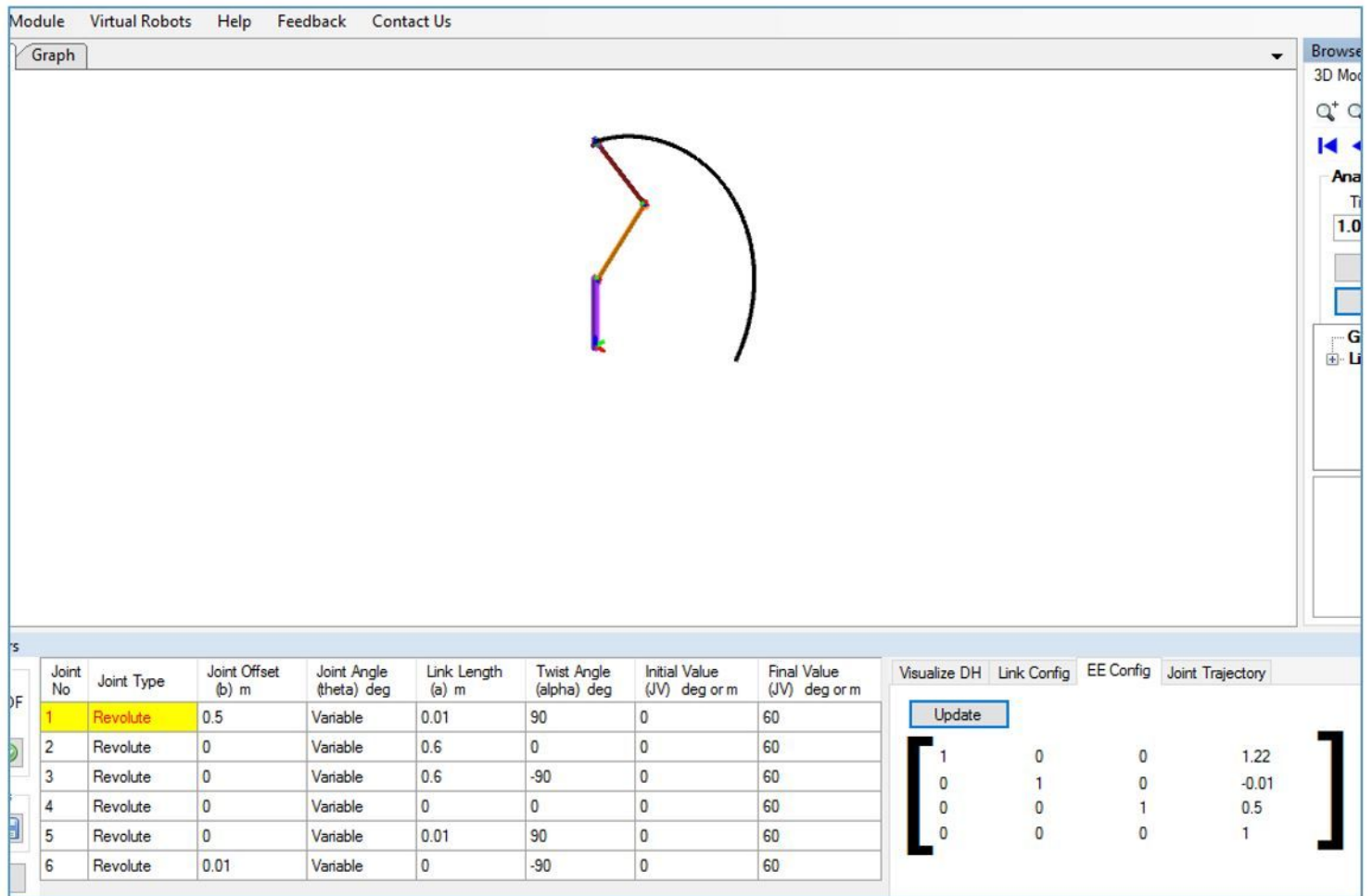


Figure 7

Forward Kinematics module in RoboAnalyzer for 6R manipulator

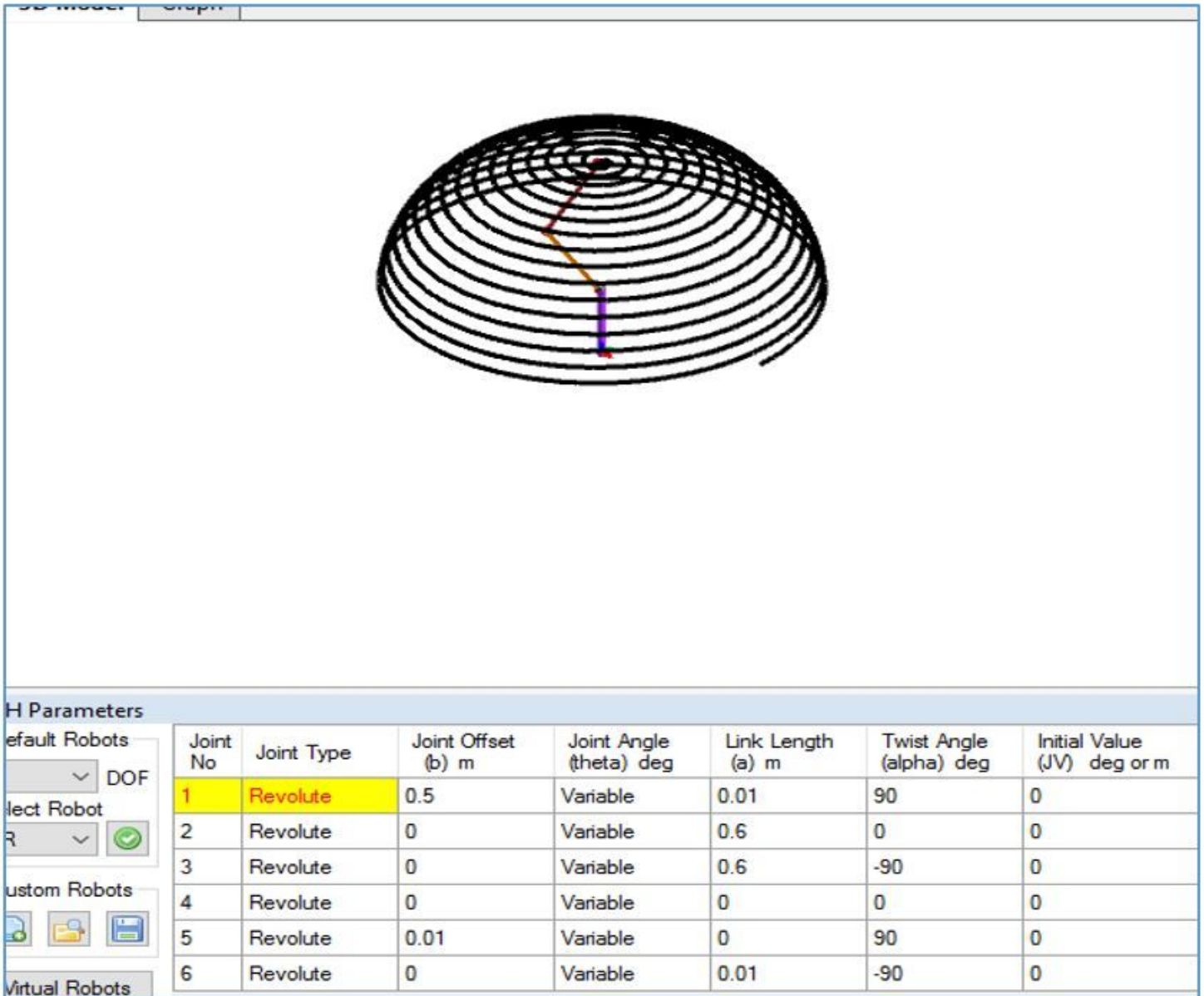


Figure 8

Workspace for the 6R manipulator on RoboAnalyzer

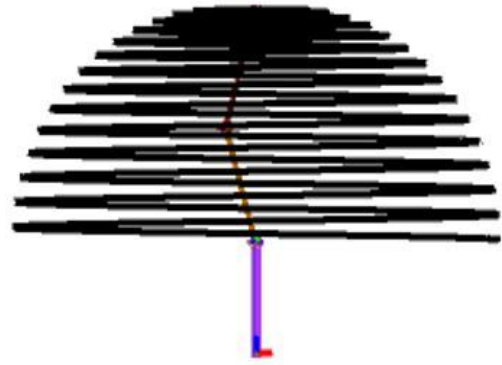
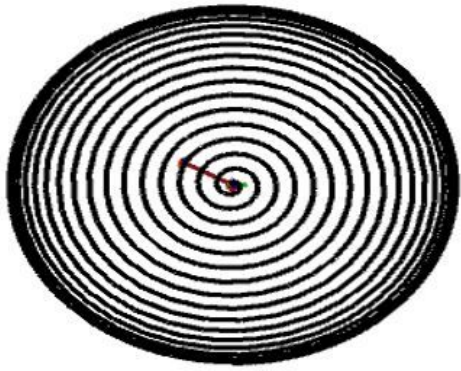


Figure 9

Top view and front view of the workspace

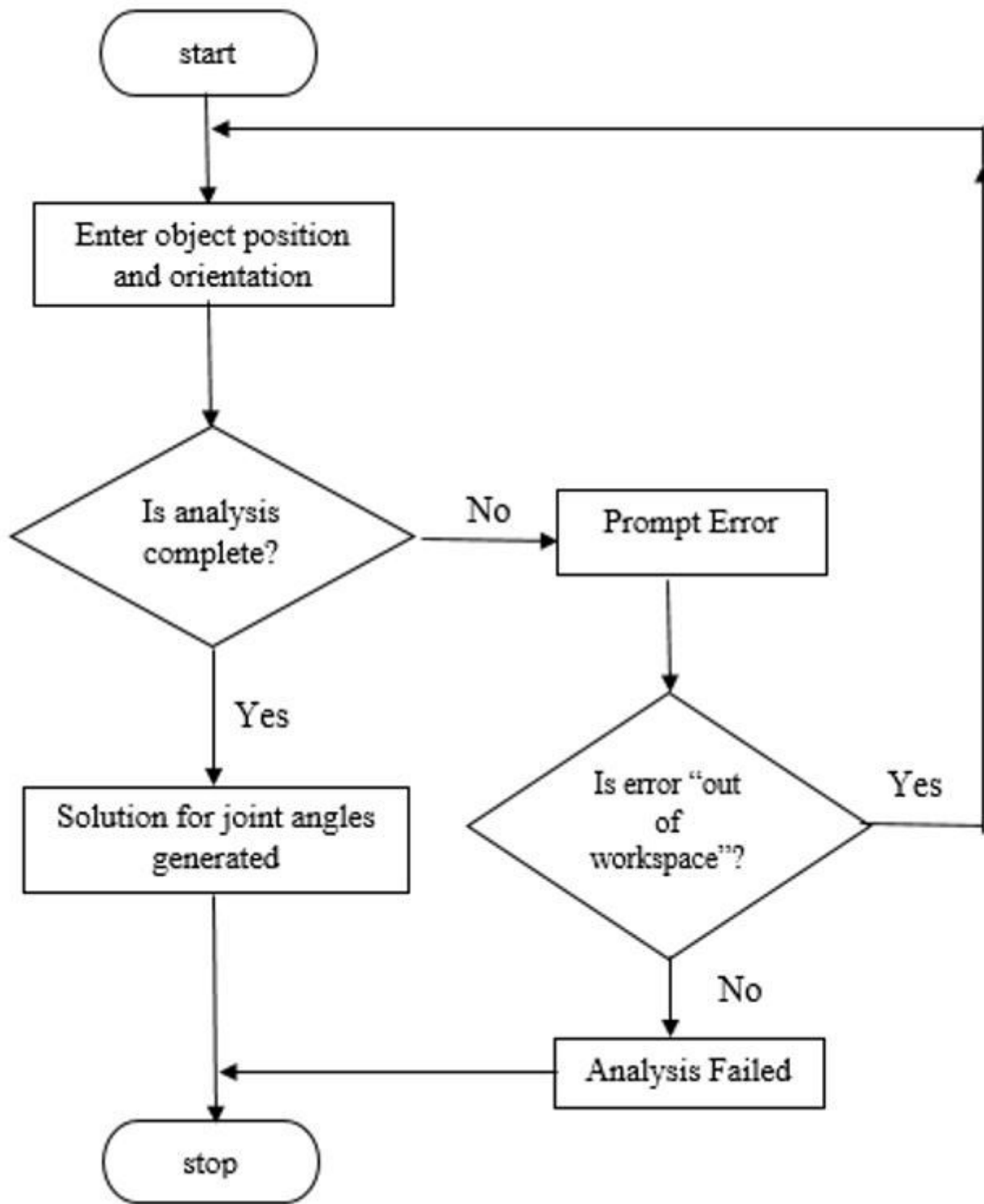


Figure 10

Inverse kinematics algorithm for RoboAnalyzer

Inverse Kinematics

Select Robot: 6R Generic Manipu ▾

Joint Offset (b) m	Link Length (a) m	Twist Angle (alpha) deg
1: 0.5	1: 0.01	1: 90
2: 0	2: 0.6	2: 0
3: 0	3: 0.6	3: -90
4: 0	4: 0	4: 0
5: 0.01	5: 0	5: 90
6: 0	6: 0.01	6: -90

End Effector's Position

X (m): 1.22
Y (m): -0.01
Z (m): 0.5

Orientation Matrix

1	0	0
0	1	0
0	0	1



IKin **Analysis Complete**

Solution	Joint 1	Joint 2	Joint 3	Joint 4	Joint 5	Joint 6	
1	-180	-180	19.946475	168.204104	175.229053	50.847342	Show
2	-180	-180	19.84951	179.921031	-178.39359	179.244173	Show
3	-180	-180	19.85142	179.926583	179.848871	-155.750364	Show
4	-180	180	24.624425	22.344106	-176.034706	164.839387	Show
5	-180	-180	24.623372	22.346785	170.889667	122.95961	Show
6	-180	-180	24.622989	22.375513	-179.991022	142.558519	Show
7	-180	19.844321	-179.997736	-179.446384	-133.843967	-0.475136	Show
8	-180	19.849558	-179.969083	177.140905	-16.520493	0.384711	Show
9	-180	19.838468	-179.970578	179.205288	-179.030109	0.914905	Show
10	180	19.849631	179.944133	-179.325212	179.999899	-0.950969	Show
11	180	19.822193	-179.821465	-179.817639	176.483136	0.580694	Show
12	180	19.850092	179.841418	179.756494	-179.999976	0.135398	Show
13	-180	19.890525	179.798657	179.148731	-179.640869	-0.960769	Show
14	-180	19.848648	-179.785116	177.925174	170.944588	-0.823668	Show
15	180	19.941556	166.428941	165.049593	-156.264691	-0.12597	Show
16	-180	19.849089	-179.887722	175.978189	-109.517917	0.087962	Show

For FKIn

Select Initial Values

Solution 1 ▾

Select Final Values

Solution 2 ▾

OK

Figure 11

Inverse Kinematic Results for the given end effector position and orientation

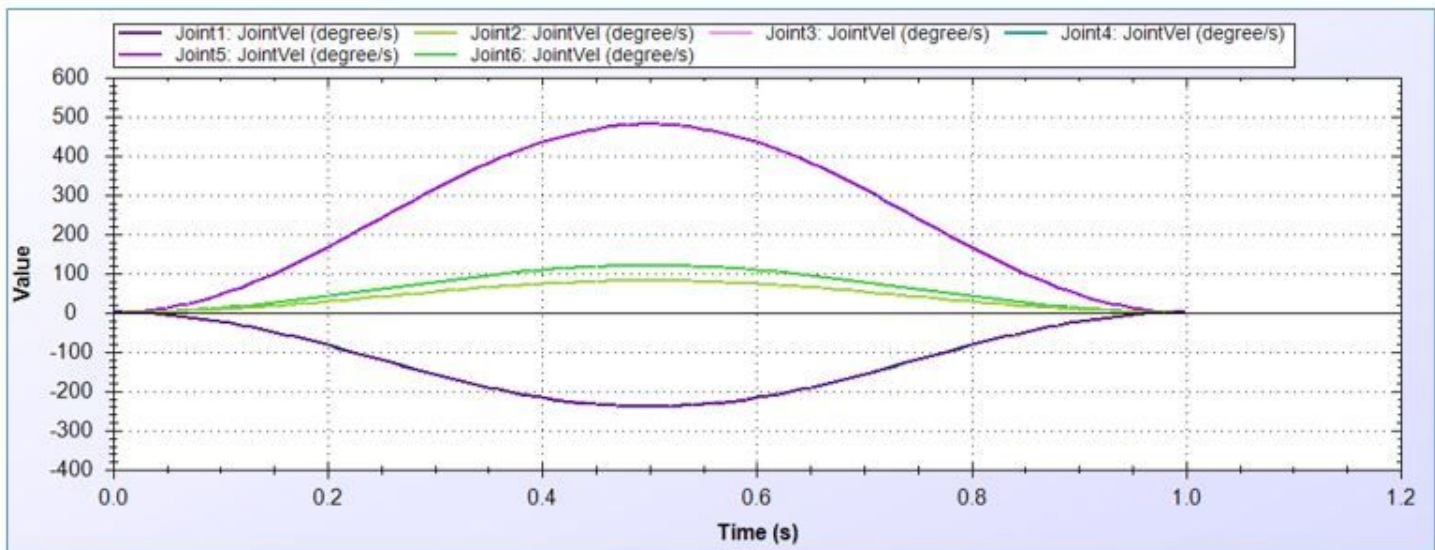


Figure 12

Comparison of all velocities of joints for 6R manipulator

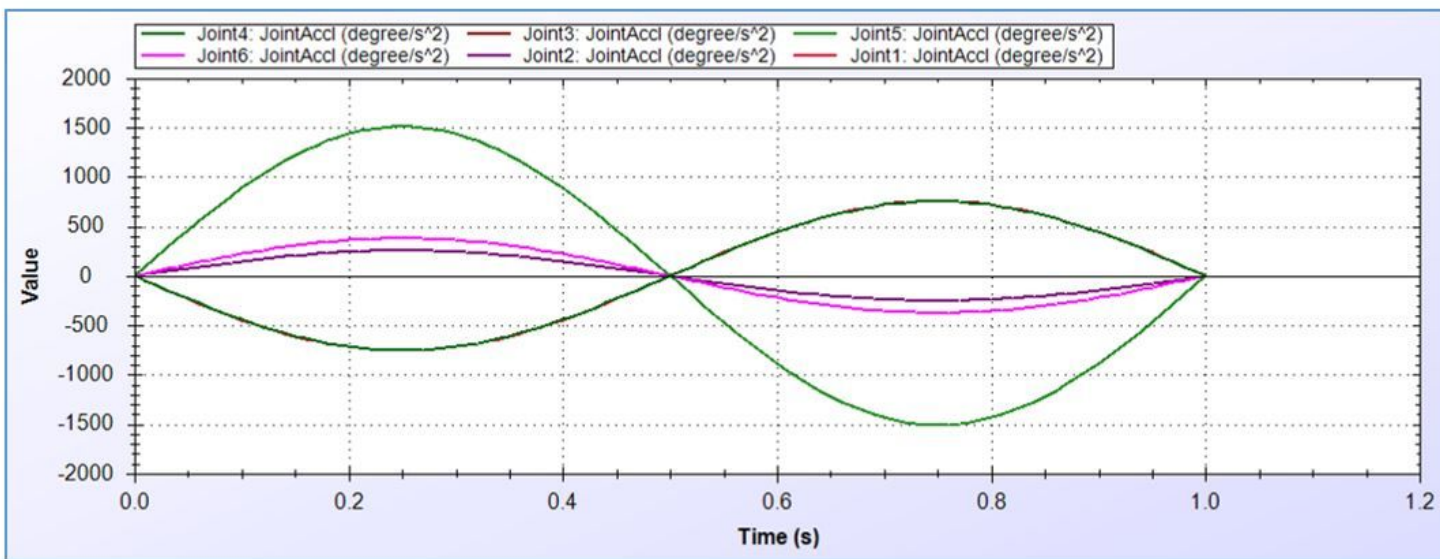


Figure 13

Comparisons of all accelerations of all 6 joints for 6R manipulator

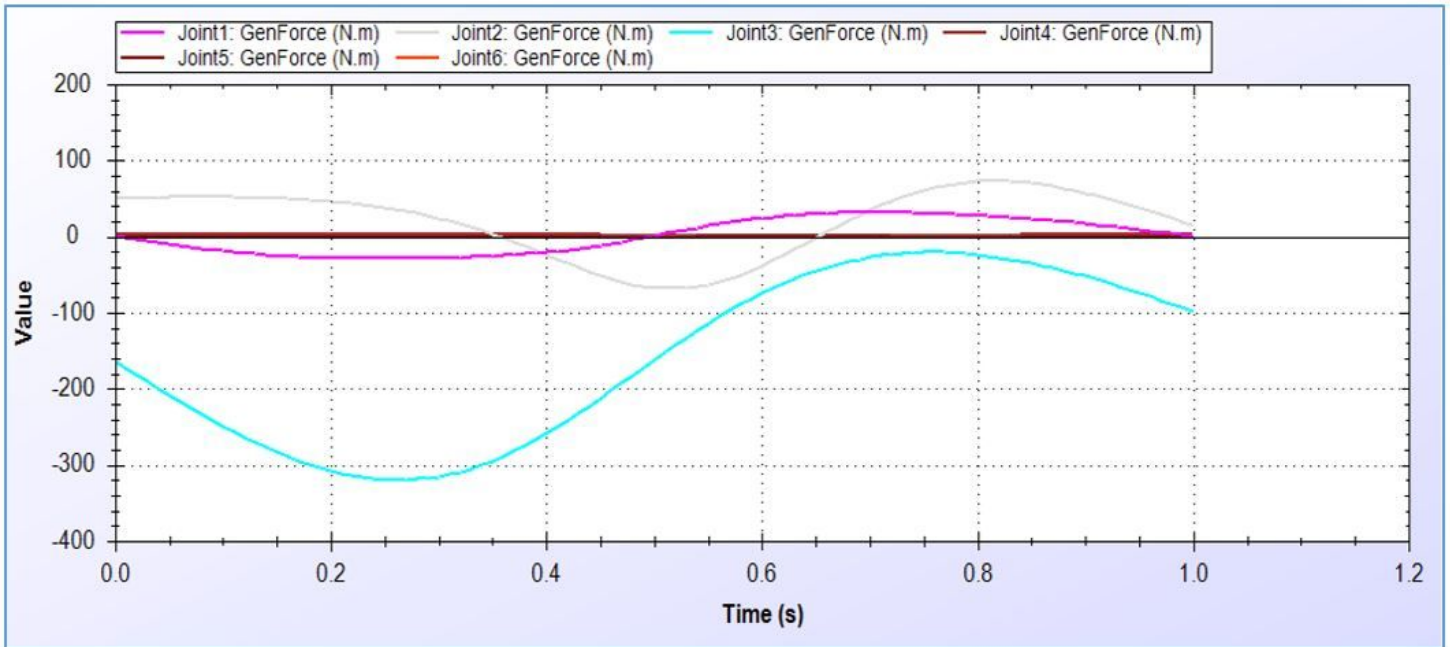


Figure 14

Comparison of torques of all joints for 6R manipulator